Zeolite Growth in Nonionic Microemulsions: Synthesis of Hierarchically Structured Zeolite Particles

Seungju Lee and Daniel F. Shantz*

Department of Chemical Engineering, Texas A&M University, 3122 TAMU, College Station, Texas 77843-3122

Received August 18, 2004. Revised Manuscript Received October 22, 2004

The synthesis of silicalite-1 in nonionic microemulsions is explored. The work presented here is a systematic study showing how parameters such as synthesis temperature, microemulsion composition, and surfactant identity impact the formation and growth of silicalite-1. The work demonstrates the possibility of using microemulsions to manipulate the shape and size of silicalite-1 materials, growing both spheres and high-aspect ratio platelets. In both cases, these large particles are robust aggregates of small submicron particles that are stable to calcination. The size of the primary particles is adjustable based on the synthesis temperature, whereas the size of the large aggregates is adjustable based on the silicalite-1 content of the mixture. On the basis of the results presented, a mechanism is proposed illustrating the role of both the confined space presented by the microemulsion as well as the importance of the surfactant−silicate interactions leading to the formation of the large aggregates. The results suggest this to be a versatile and useful approach for making zeolitic materials that possess unique morphological properties and hierarchical structure.

Introduction

Zeolites are crystalline, microporous (alumino) silicates that have been extensively used in heterogeneous catalysis, separations, and ion-exchange operations.[1,2] It has long been understood that particle size and morphology play a central role in the successful application of zeolites in the areas of catalysis and separations.[3−7] This is particularly acute in catalytic applications where the particle size can have a dramatic effect on the product distribution due to differences in rates of transport/diffusion and reaction. There have been numerous studies of how one can control the particle size of zeolites through a variation of synthesis conditions.[8] In general terms, the zeolite science community has developed approaches to make both very small (<500 nm) and very large (>50 μm) crystals of many zeolitic materials including low-silica phases such as zeolites X, A, and L and high-silica phases such as a beta and various MFI materials (Al-ZSM-5, silicalite-1, TS-1).[8−18]

By contrast, manipulating the morphology of zeolite crystals is poorly understood. A notable exception is work by Beck and Davis showing that different structure-directing agents (SDAs) could be used to manipulate the morphology of submicron sized silicalite-1 particles.[19] Lai and co-workers showed that oriented silicalite-1 thin films with superior sieving properties could be obtained by using these different SDAs in secondary growth,[20] demonstrating the potential applications available if one could control zeolite morphology. While using different SDAs is a very attractive approach, it may not be a general one. However, Lai's work clearly demonstrates the breakthroughs that lie ahead if one could develop a means to manipulate the morphology of zeolite crystals. Such materials could find use as novel adsorbents or catalysts, be integrated into microdevices, be utilized as templates for growing high-density arrays of carbon nanotubes or metal nanowires, or used in thin film formation.

* Corresponding author. Phone: (979) 845-3492. Fax: (979) 845-6446. E-mail: shantz@che.tamu.edu.

(1) Barrer, R. M. *Hydrothermal Chemistry of Zeolites*; Academic Press: London, 1982.
(2) Breck, D. W. *Zeolite Molecular Sieves*: *Structure, Chemistry and Use*; Wiley: New York, 1974.
(3) Csicsery, S. M. *Zeolites* **1984**, *4*, 202−213.
(4) Chen, N. Y.; Degnan, T. F. J.; Smith, C. M. *Molecular Transport and Reaction in Zeolites* : *Design and Application of Shape Selective Catalysts*; VCH: New York, 1994.
(5) Corma, A. *J. Catal*. **2003**, *216*, 298−312.
(6) *Catalysis and Zeolites*: *Fundamentals and Applications*; Weitkamp, J., Puppe, L., Eds.; Springer-Verlag: Berlin, 1999.
(7) Wojciechowski, B. W.; Corma, A. *Catalytic Cracking*: *Catalysis, Chemistry, and Kinetics*; Dekker: New York, 1986.
(8) *Zeolite Synthesis*; Karge, H. G., Weitkamp, J., Eds.; Springer-Verlag: Berlin, 1998.
(9) Cundy, C. S.; Forrest, J. O.; Plaisted, R. J. *Micropor. Mesopor. Mater*. **2003**, *66*, 143−156.
(10) Holmberg, B. A.; Wang, H. T.; Norbeck, J. M.; Yan, Y. S. *Micropor. Mesopor. Mater*. **2003**, *59*, 13−28.
(11) Mintova, S.; Olson, N. H.; Valtchev, V.; Bein, T. *Science* **1999**, *283*, 958−960.
(12) Persson, A. E.; Schoeman, B. J.; Sterte, J.; Ottesstedt, J. E. *Zeolites* **1994**, *14*, 557−567.
(13) Tsapatsis, M.; Lovallo, M.; Davis, M. E. *Microporous. Mater*. **1996**, *5*, 381−388.
(14) Zhu, G. S.; Qiu, S. L.; Yu, J. H.; Sakamoto, Y.; Xiao, F. S.; Xu, R. R.; Terasaki, O. *Chem. Mater*. **1998**, *10*, 1483−1486.
(15) Shimizu, S.; Hamada, H. *Micropor. Mesopor. Mater*. **2001**, *48*, 39−46.
(16) Sun, Y. Y.; Song, T.; Qiu, S.; Pang, W.; Shen, J.; Jiang, D.; Yue, Y. *Zeolites* **1995**, *15*, 745−753.
(17) Charnell, J. F. *J. Cryst. Growth* **1971**, *8*, 291−294.
(18) Gao, F. F.; Zhu, G. S.; Li, X. T.; Li, B. S.; Terasaki, O.; Qiu, S. L. *J. Phys. Chem. B* **2001**, *105*, 12704−12708.
(19) Beck, L. W.; Davis, M. E. *Micropor. Mesopor. Mater*. **1998**, *22*, 107−114.
(20) Lai, Z. P.; Bonilla, G.; Diaz, I.; Nery, J. G.; Sujaoti, K.; Amat, M. A.; Kokkoli, E.; Terasaki, O.; Thompson, R. W.; Tsapatsis, M.; Vlachos, D. G. *Science* **2003**, *300*, 456−460.

10.1021/cm0486114 CCC: $30.25
Published on Web 01/04/2005

Another approach is to use microemulsions as confined spaces or nanoreactors for zeolite growth, as has been shown to be very successful in the synthesis of metal, metal oxide, and metal sulfide nanoparticles.[21−26]There are relatively few reports in the literature that have studied the formation and growth of zeolites in the presence of a microemulsion. Dutta and co-workers have studied the nucleation of zeolite A and the zincophosphate analogues of sodalite and faujasite in microemulsions, although controlling morphology was not the goal of their studies.[27−29] Yates and colleagues have recently employed cationic microemulsions for the synthesis of $ALPO_4$-5 fibrils and tetrapods.[30−32] The only previous report of all-silica zeolites formed in microemulsions was by Manna et al. on fluoride-mediated MFI syntheses in AOT microemulsions.[33] On the basis of the limited literature in this area, we have focused our efforts on using microemulsions for manipulating zeolite particle morphology. There are two balancing or competing factors in this approach. On one hand, the microemulsion constitutes a confined space that will potentially modulate nucleation and growth (nanoreactor). On the other hand, the surfactant will coordinate to the crystallographic faces of the growing crystal and affect the growth rates depending on the crystallographic orientation of the surface and the strength of the organic−inorganic interactions. The latter effect should be tunable in a rational manner by changing the chemical nature of the surfactant. A key issue in determining the formation and growth of microporous materials in microemulsions is the nature and strength of the interactions between the surfactants forming the microemulsion and the zeolite particles or silicate precursors. Given the complexity of this process, here we have chosen to analyze the formation and growth of silicalite-1 from so-called clear-solution syntheses made in the presence of nonionic microemulsions. This zeolite synthesis was chosen due to its simplicity as it contains only water, tetraethyl orthosilicate (TEOS), and tetrapropylammonium hydroxide (TPAOH), and also because it has been extensively studied.[9,12,34−47] Another advantage of this system is that given the low temperatures employed, the phase behavior of the zeolite−microemulsion mixtures can be directly determined.

Several factors led us to choose nonionic microemulsions for this work. First, the phase behavior and solubility of nonionic surfactants has been extensively studied, particularly under the conditions of equal amounts of water and oil.[48−51]In these systems, one can observe the fish shape of the phase diagram as a function of temperature. At intermediate surfactant concentrations, the mixtures change from a Winsor type I system to an isotropic microemulsion as the temperature is increased. At higher temperatures and the same concentrations, the isotropic microemulsion phase separates into two phases, both of Winsor type II. At lower surfactant concentrations, the phase behavior evolves from a Winsor type I system to a Winsor type II system via a Winsor type III as temperature increases. In the view of solubility, nonionic surfactants are more soluble in water at lower temperature but more soluble in oil at higher temperature.[52] Also, in contrast to ionic surfactants, no additional ions are introduced into the system. This avoids any possible ion effects on nucleation and growth, again with the aim of keeping the system as simple as possible. Also, the surfactant−silicalite interactions should be relatively weak. Finally, as noted previously, the solubility of nonionic surfactants (and subsequently the phase behavior) is known to be strongly temperature dependent, allowing us to study how this may impact material formation.

We have recently reported preliminary results on the growth of silicalite-1 crystals in nonionic microemulsions.[53] The work presented here expounds in detail on our previous report, showing how parameters such as synthesis temperature, microemulsion composition, and surfactant identity impact the formation and growth of silicalite-1. The results presented demonstrate the ability to manipulate the shape and size of silicalite-1 materials, growing both spheres and high-aspect ratio platelets. In both cases, these large particles are robust aggregates of small submicron particles that are stable to calcination. The size of the primary particles is adjustable based on the synthesis temperature, whereas the size of the large aggregates is adjustable based on the silicalite-1 content of the mixture. On the basis of the results

(21) Althues, H.; Kaskel, S. *Langmuir* **2002**, *18*, 7428−7435.
(22) Chang, C.; Fogler, H. S. *Langmuir* **1997**, *13*, 3295−3307.
(23) Osseo-Asare, K.; Arrigagada, F. J. *Colloids Surf.* **1990**, *50*, 321−339.
(24) Tartaj, P.; De Jonghe, L. C. *J. Mater. Chem.* **2000**, *10*, 2786−2790.
(25) Zarur, A. J.; Hwu, H. H.; Ying, J. Y. *Langmuir* **2000**, *16*, 3042−3049.
(26) Pileni, M. P. *Langmuir* **1997**, *13*, 3266−3276.
(27) Dutta, P. K.; Robins, D. *Langmuir* **1991**, *7*, 1048−1050.
(28) Dutta, P. K.; Jakupca, M.; Reddy, K. S. N.; Salvati, L. *Nature* **1995**, *374*, 44−46.
(29) Singh, R.; Doolittle, J.; George, M. A.; Dutta, P. K. *Langmuir* **2002**, *18*, 8193−8197.
(30) Yates, M. Z.; Ott, K. C.; Birnbaum, E. R.; McCleskey, T. M. *Angew. Chem. Int. Ed.* **2002**, *41*, 476−478.
(31) Lin, J.-C.; Dipre, J. T.; Yates, M. Z. *Chem. Mater.* **2003**, *15*, 2764−2773.
(32) Lin, J.-C.; Dipre, J. T.; Yates, M. Z. *Langmuir* **2004**, *20*, 1039−1042.
(33) Manna, A.; Kulkarni, B. D.; Ahedi, R. K.; Bhaumik, A.; Kotasthane, A. N. *J. Coll. Int. Sci.* **1999**, *213*, 405−411.
(34) Mintova, S.; Olson, N. H.; Senker, J.; Bein, T. *Angew. Chem. Int. Ed.* **2002**, *41*, 2258−2561.
(35) Cundy, C. S.; Lowe, B. M.; Sinclair, D. M. *J. Cryst. Growth* **1990**, *100*, 189−202.
(36) Mintova, S.; Valtchev, V. *Micropor. Mesopor. Mater.* **2002**, *55*, 171−179.
(37) Mintova, S.; Valtchev, V.; Bein, T. *Coll. Surf. A* **2003**, *217*, 153−157.
(38) Nikolakis, V.; Kokkoli, E.; Tirrell, M.; Tsapatsis, M.; Vlachos, D. G. *Chem. Mater.* **2000**, *12*, 845−853.
(39) Nikolakis, V.; Tsapatsis, M.; Vlachos, D. G. *Langmuir* **2003**, *19*, 4619−4626.
(40) Schoeman, B. J.; Sterte, J.; Otterstedt, J. E. *Zeolites* **1994**, *14*, 568−575.
(41) Schoeman, B. J.; Regev, O. *Zeolites* **1996**, *17*, 447−456.
(42) Schoeman, B. J. *Micropor. Mesopor. Mater.* **1997**, *9*, 267−271.
(43) Schoeman, B. J. *Zeolites* **1997**, *18*, 97−105.
(44) Schoeman, B. J. *Microporous Mesoporous Mater.* **1998**, *22*, 9−22.
(45) Watson, J. N.; Iton, L. E.; Keir, R. I.; Thomas, J. C.; Dowling, T. L.; White, J. W. *J. Phys. Chem. B* **1997**, *101*, 10094−10104.
(46) Yang, S.; Navrotsky, A. *Chem. Mater.* **2002**, *14*, 2803−2811.
(47) Yang, S.; Navrotsky, A.; Wesolowski, D.; Pople, J. A. *Chem. Mater.* **2004**, *16*, 210−219.
(48) Friberg, S.; Lapczynska, I. *Prog. Coll. Polym. Sci.* **1975**, *56*, 16−20.
(49) Kahlweit, M.; Strey, R. *Angew. Chem. Int. Ed.* **1985**, *24*, 654−668.
(50) Kahlweit, M.; Strey, R.; Busse, G. *J. Phys. Chem.* **1990**, *94*, 3881−3894.
(51) Schubert, K.-V.; Kaler, E. W. *Ber. Bunsen-Gens. Phys. Chem.* **1996**, *100*, 190−205.
(52) Kahlweit, M.; Strey, R.; Firman, P. *J. Phys. Chem.* **1986**, *90*, 671−677.
(53) Lee, S.; Shantz, D. F. *Chem. Commun.* **2004**, 680−681.

presented, a mechanism is proposed illustrating the role of both the confined space presented by the microemulsion as well as the importance of the surfactant−silicate interactions leading to the formation of the large aggregates. Our results suggest this to be a versatile and useful approach for fabricating complex zeolitic materials that possess unique morphological properties and hierarchical structure.

Experimental Procedures

Materials. Nonionic surfactants, Igepal CO-520, CO-720, and CO-890, were used as received from Aldrich. These surfactants are polydisperse mixtures of polyoxyethylene(*x*)nonylphenyl ethers with mean ethoxylation degrees of 5 (CO-520), 12 (CO-720), and 40 (CO-890). Tetraethyl othosilicate, TEOS (99+% Aldrich), reagent grade heptane and butanol (VWR), and tetrapropylammonium hydroxide, TPAOH (40% w/w Alfa Aesar), were used as received.

Phase Behavior. Phase diagrams for the heptane/water/IGEPAL/butanol systems were determined over the temperature range of 298−368 K. The one-phase two-phase envelopes of mixtures where the water was replaced by an equivalent amount of silicalite-1 synthesis mixture (by weight) have also been determined. The silicalite-1 mixture has a molar composition of 1 TEOS:0.36 TPAOH:20 H_2O. Unless stated otherwise, the IGEPAL/butanol weight ratio was fixed at 2:1. In the Results, mixture compositions are described using weight fractions with the following notation: H−heptane, S−Igepal + butanol, and M−silicalite-1 mixture. As an example, 0.2:0.6:0.2 H−S−M is 20% weight in heptane, 60% weight in Igepal and butanol, and 20% weight in silicalite-1 mixture. This information, along with the Igepal/butanol ratio and temperature, specify the system.

Zeolite Synthesis. Zeolite samples grown in oil/water/surfactant mixtures were prepared as follows: fixed amounts of heptane, surfactant, and butanol were mixed together in a Pyrex screw-cap test tube at room temperature. The corresponding amounts of TPAOH, deionized water, and TEOS were then added sequentially. The test tubes were then closed and vigorously shaken for 5 min, at which point they were placed in an oven at the desired temperature and allowed to react under quiescent conditions for a given period of time. Test tubes used in synthesis were typically 50−60% full (by volume) at room temperature. Unless stated otherwise, the synthesis duration was 96 h. Samples were collected by filtration, washed with copious quantities of ethanol, acetone, and water, and air-dried.

Characterization. Powder X-ray diffraction (PXRD) measurements were performed using a Bruker D-8 X-ray diffractometer with CuKα radiation. Samples were analyzed over a range of 0.8−30° 2θ using a step scan mode with a step size of 0.04° and a step rate of 3 s/step. Peak intensities and 2θ values were determined using the Bruker program EVA. Field-emission scanning electron microscopy (FE-SEM) measurements were performed using a Zeiss Leo-1530 microscope operating at 1−10 kV. The microscope employs a GEMINI electron optical column with a Schottky-type field emitter, single condenser, crossover-free beam path, large specimen chamber with two chamber ports for EDS or WDS adaptation, four accessory ports on the chamber and three on the door, fail-safe vacuum system, digital image store, and processor. Nitrogen adsorption experiments were performed on a Micromeritics ASAP 2010 micropore analyzer with a turbopump capable of obtaining relative pressures of less than 10^{-6}. The samples used in adsorption experiments were calcined to remove the TPAOH by being heated from room temperature to 723 K at a rate of 1 K/min and were then heated at 723 K for 8 h. Samples used in the adsorption measurements were degassed at 373 K for 4 h, then at 573 K overnight before the measurements were performed. The isotherms were measured over the relative pressure range of 10^{-6} to 0.98. The micropore volume was determined using the α_s-method.[54,55] Dynamic light scattering measurements were carried out using a ZetaPals instrument from Brookhaven Instruments. Transmission electron microscopy (TEM) was performed on a JEOL 2010 microscope with a lanthanum hexaboride filament and an excitation voltage of 200 kV. The samples were mortared and pestled and then dispersed in ethanol (100%, Aldrich) and placed on a 400-mesh copper grid.

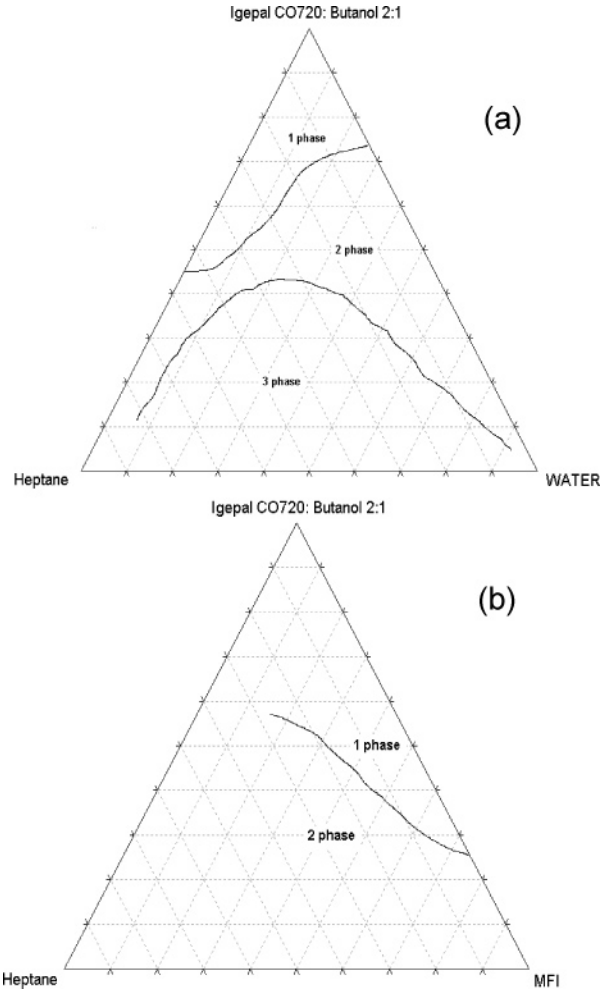

Figure 1. Phase behavior of the heptane/Igepal CO-720/butanol/water (a) and heptane/Igepal CO-720/butanol/silicalite-1 (b) mixtures at 353 K. Igepal CO-720 to butanol ratio is 2:1.

Results

Phase Behavior. Figure 1 shows the phase diagram for the heptane/CO-720/butanol/water (a) and heptane/CO-720/butanol/silicalite-1 (b) mixtures at 353 K. For simplicity, the surfactant and cosurfactant are lumped together, and the zeolite mixture is treated as one component so the system can be visually represented on a ternary phase diagram. The phase behavior was determined between 353 and 368 K. As shown in Figure 1a, the one-phase region is located in the

(54) Gregg, S. J.; Sing, K. S. W. *Adsorption, Surface Area, and Porosity*; Academic Press: London, 1982.
(55) Rouquerol, F.; Roquerol, J.; Sing, K. *Adsorption by Powders and Porous Solids*; Academic Press: San Diego, 1999.

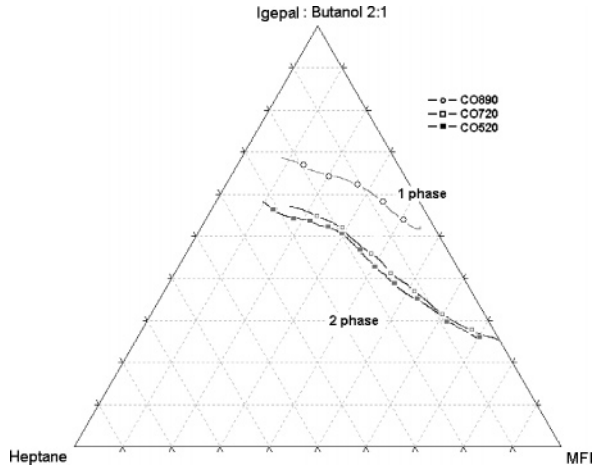

Figure 2. Phase behavior of heptane/Igepal + butanol/silicalite-1 at 353 K.

high surfactant region, and the three-phase region is found in the low surfactant region with the two-phase region in between. Figure 1a shows that the phase boundary extends from the point 25% heptane, 55% surfactant to the point 73% heptane, 27% surfactant and that the one-phase region is located in the lower heptane region. Upon replacing the water with an equivalent amount (by weight) of silicalite-1 mixture, the phase boundary shifts toward the lower heptane region. One possibility for this behavior is that the large quantity of ethanol formed during TEOS hydrolysis (~10 mol of ethanol/L of water) acts as a cosurfactant. A series of nonionic surfactants has also been studied to determine how the number of EO units in the hydrophilic headgroup influences the phase behavior, while keeping the hydrophobic tail the same. The one-phase/two-phase envelopes at 353 K are shown in Figure 2 and indicate that the one-phase region decreases in size as the EO headgroup increases. Increasing the number of EO units in the headgroup makes the surfactants more soluble in water, similar to the effect of decreasing the temperature. As stated in the Introduction, two-phase mixtures with an oil-excess phase and oil-in-water microemulsion phase (Winsor type I) can be obtained from a one-phase mixture with decreasing temperature or increasing headgroup size. The results shown in Figure 2 where the one-phase/two-phase envelope shifts to higher surfactant contents for the IGEPAL 890 can be understood on this basis.

Particle Morphology. Figure 3 shows the FE-SEM and powder X-ray diffraction (PXRD) data for a sample of silicalite-1 made in a microemulsion of composition 0.2:0.6:0.2 H−S−M (Igepal CO-720) at 353 K. The particles formed are spherical and 3−5 μm in diameter. The peaks present in the PXRD data are consistent with those of silicalite-1; however, they are much broader than what one would expect from crystals larger than one micron in size. TEM on this sample (Figure 4) shows that the large spheres are actually aggregates of particles that are between 10 and 30 nm in size. These spheres are stable to calcination as is observed in Figure 3, as no differences are observed before and after calcination in the PXRD and FE-SEM results. The micropore volume of this sample is 0.10 cm^3/g as determined by nitrogen adsorption. On the basis of TEM and PXRD, the spheres are silicalite-1 with very little or no amorphous

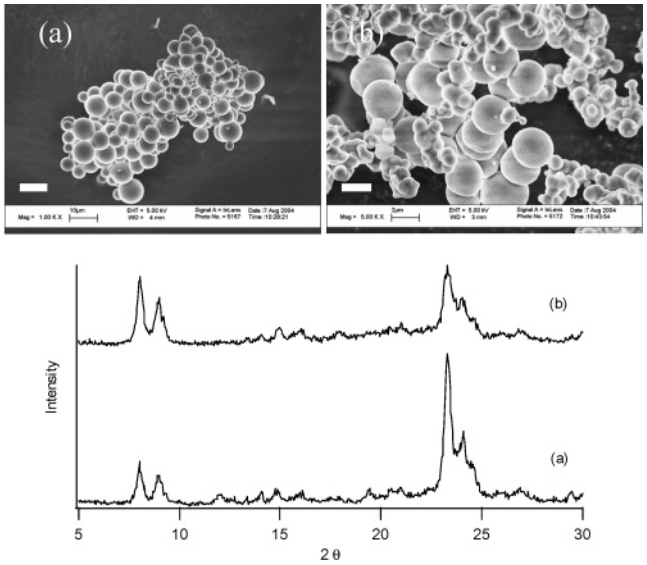

Figure 3. FE-SEM and PXRD data of (a) as-made and (b) calcined samples formed from mixtures of composition 0.2:0.6:0.2 (H−S−M, Igepal CO-720) at 353 K. Scale bars are (a) 10 μm and (b) 2 μm.

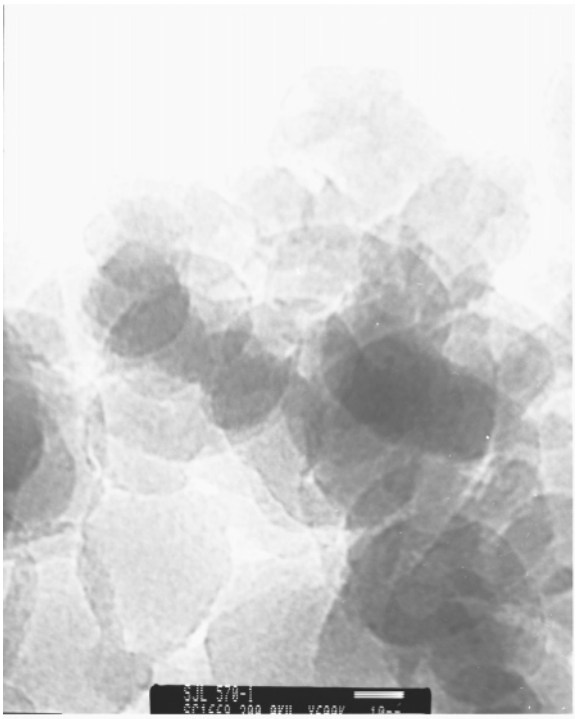

Figure 4. TEM of sample shown in Figure 3. Scale bar is 10 nm.

impurities present. Moreover, spheres are obtained over a wide range of compositions but preferably in the one-phase region between 45 and 65% surfactant. However, in syntheses where low heptane contents (below 10%) or low silicalite-1 mixture contents (less than 15%) are employed, spherical particles are not obtained (Supporting Information).

It is also observed that the size of the large spherical particles is controllable based on the weight fraction of the silicalite-1 mixture. Figure 5 shows the FE-SEM images of spherical particles made as the weight fraction of silicalite-1 mixture is varied. These materials are all silicalite-1 by PXRD. The particle size changes from approximately 3−5 μm (0.2:0.6:0.2 H−S−M) to 6−10 μm (0.2:0.4:0.4 H−S−M) at 353 K for the CO-720 system. The micropore

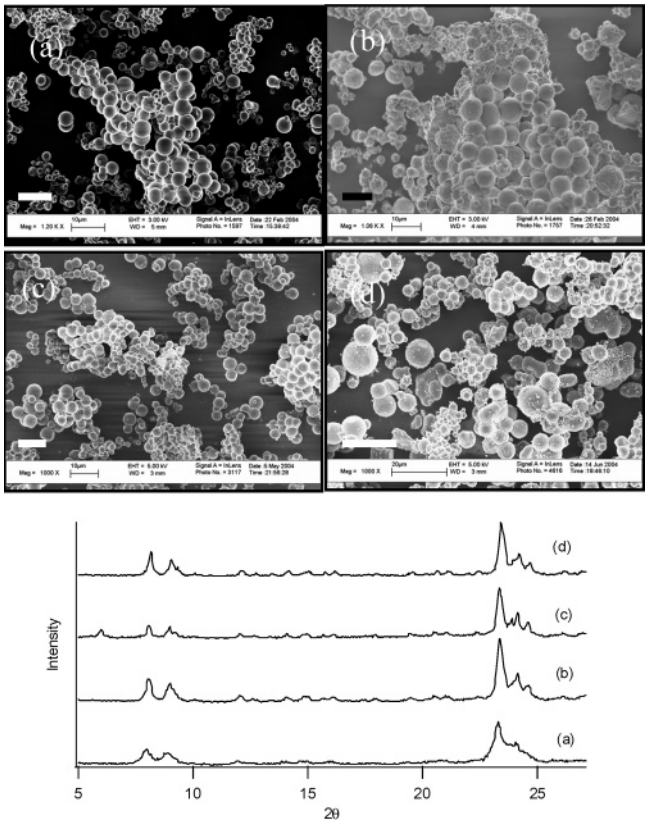

Figure 5. FE-SEM and PXRD data of silicalite-1 made from mixtures of composition (a) 0.2:0.6:0.2 and (b) 0.2:0.4:0.4 H−S−M at 353 K and (c) 0.15:0.6:0.25 and (d) 0.15:0.45:0.4 H−S−M at 368 K. Scale bars are (a−c) 10 μm and (d) 20 μm.

volumes of these samples are 0.10 and 0.14 cm^3/g as determined by nitrogen adsorption, respectively. Dynamic light scattering measurements on dilute (0.1 wt %) suspensions of particles verify the results from the FE-SEM images. The FE-SEM images show that an increase in the particle size is observed as the surfactant content is decreased and the silicalite-1 content is increased. In all cases, a spherical morphology is obtained, even though the 0.2:0.4:0.4 H−S−M mixture phase separates at 353 K. Moreover, by PXRD, the crystallinity is observed to improve as the aqueous fraction increases and the surfactant fraction decreases. The particle size change is similar at 368 K: 3−5 μm (0.15:0.6:0.25 H−S−M) to 6−10 μm (0.15:0.45:0.4 H−S−M). That the size of the spheres is insensitive to temperature is in contrast to zeolite growth in conventional syntheses, where the particle size is usually strongly a function of temperature. Another point to note is that the surfaces of the spheres change as the microemulsion composition is varied. Figure 6 shows FE-SEM and PXRD of samples made at 353 K at different microemulsion compositions. As can be seen, the samples made at lower surfactant content (0.4 weight fraction) have rougher surfaces as compared to samples made at higher surfactant content (0.6 weight fraction). These results suggest that the surfactant plays a role in controlling the surface smoothness (i.e., the primary particle size) of the large particles obtained.

In addition to spherical particles, platelets of silicalite-1 can also be formed. Figure 7 shows the FE-SEM of platelets at high and low magnification, as well as the PXRD pattern

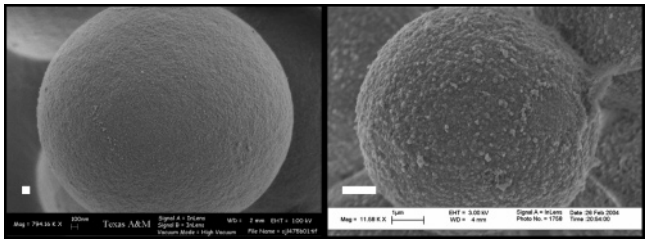

Figure 6. FE-SEM images of silicalite-1 made from mixtures of composition (a) 0.2:0.6:0.2 and (b) 0.2:0.4:0.4 (H−S−M, Igepal CO-720) at 353 K. Scale bars are (a) 100 nm and (b) 1 μm.

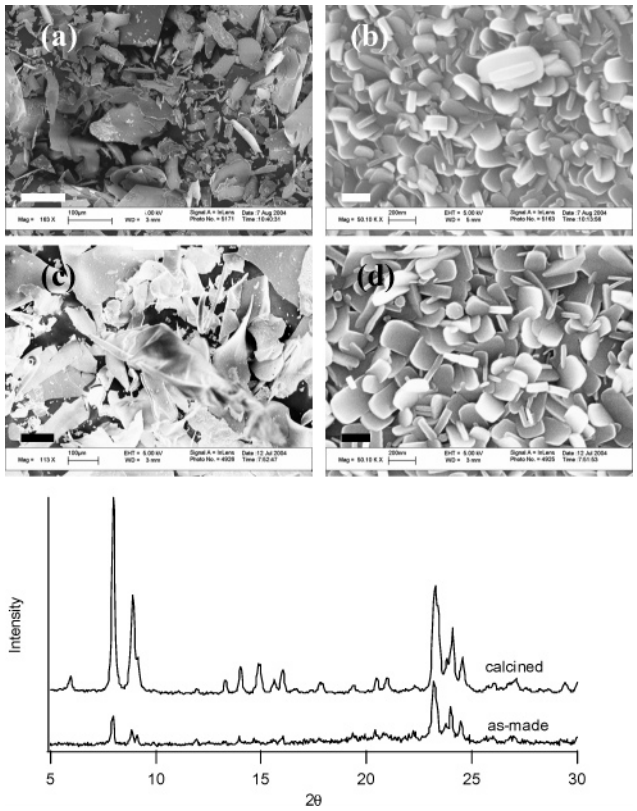

Figure 7. FE-SEM and PXRD of platelike silicalite-1 (a), (b) as-made, and (c and d) calcined samples from mixtures of composition 0.58:0.34:0.08 H−S−M Igepal CO-520, surfactant/butanol 1:1 at 368 K. Scale bars are (a and c) 100 μm and (b and d) 200 nm.

for the sample. The large (>50 μm) platelets are aggregates of small (300 nm) particles. It is also noteworthy that the primary particles have a much better defined coffin-like morphology as compared to those made under the same conditions without the microemulsion, which are typically irregularly spherical possessing a rough surface.[46] In contrast to the spherical samples, it is much more difficult to make platelets that show no amorphous phase by PXRD. Reproducibility is more problematic in the growth of plates as compared to spheres, consistent with the observation that plates are formed in a much narrower composition space as compared to the spheres. Plate-shape particles are made in the low silicalite-1 region (around 0.58:0.34:0.08 H−S−M) by using CO-520 at 368 K. The phase inversion temperature (PIT) of CO-520 (HLB number 10) is approximately 300 K,[48] well below the synthesis temperature. Under these conditions, the mixture is initially two phases but after 4 days at 368 K becomes one phase. The platelets are also

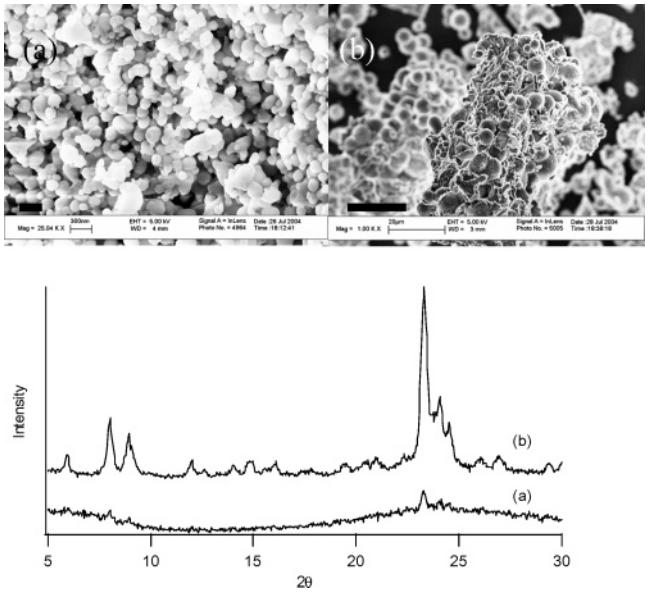

Figure 8. FE-SEM (top) and PXRD (bottom) of solids extracted from (a) bulk solution and (b) the wall of the synthesis container 38 h after synthesis at 353 K. Mixture composition 0.2:0.6:0.2 H−S−M, Igepal CO720. Scale bars are (a) 300 nm and (b) 20 μm.

stable to calcination, as observed by FE-SEM and PXRD (Figure 7). The micropore volume of the calcined platelets is 0.11 cm^3/g as determined by nitrogen adsorption.

The results outlined previously clearly show that the presence of the microemulsion leads to materials with significantly different properties as compared to silicalite-1 made with this mixture (1 TEOS:0.36 TPAOH:20 H_2O) when the microemulsion is not present. In that case, silicalite-1 particles below 300 nm are typically obtained.[9,12,34,44,46] Next, we describe how various synthesis parameters impact material properties and also propose a mechanism to explain the formation of the spheres and platelets.

Primary Particle Growth and Coalescence. A key point to understanding material growth in this system is ascertaining whether the nanoreactor concept is valid in this system or if surfactant adsorption is the dominant process. To study this, we have attempted to extract solids from the isotropic microemulsions before the onset of large particle formation, which is typically first observed after approximately 36 h at 353 K. Using the salt-out procedure described elsewhere,[56] we were not able to obtain solid materials from these mixtures before 38 h. However, Figure 8 shows the solids extracted from these mixtures after 38 h, both from the bulk solution and the solids formed on the wall of the glass test tubes used for synthesis. The results are striking: the particles in the clear solution are on the order of 100 nm in size, and primarily amorphous, although a few weak reflections for the silicalite-1 phase are observed. By contrast, the materials collected from the walls are large particles very similar to those observed from samples recovered after 96 h. This result suggest two points: first, the large particles appear to form as a result of interactions with the glass surface, and the bulk solution appears to act as the reservoir for the small particles that comprise the large particles. Consistent with this, syntheses performed in Teflon-lined autoclaves with a glass slide in the bottom lead to the formation of spherical silicalite-1 particles on the glass slide; however, the large aggregates from the bulk solution are not spherical (Supporting Information). To check the possibility that the Pyrex test tube acts as a second silica source, experiments were performed where the TEOS was removed from the synthesis mixture and replaced with 4 equiv of ethanol. From this experiment, we obtained a small amount of amorphous silica. This result shows that the Pyrex test tubes are not the silica source for the silicalite-1 obtained. Also consistent with this, syntheses performed in Teflon containers lead to the formation of silicalite-1; however, the large aggregates are not spherical (Supporting Information). From this result, it appears that having a surface from which to nucleate the large spheres is essential for their formation, and we hypothesize that the presence of the surfactant is essential for aggregate formation (i.e., large sphere formation necessitates both the glass surface and the microemulsion).

To try and resolve the issue of the nanoreactor concept, we performed numerous small-angle X-ray scattering (SAXS) and dynamic light scattering (DLS) measurements of the bare microemulsions and the synthesis mixtures. The DLS measurements were inconclusive given the high surfactant content of the mixtures. The SAXS measurements of the bare microemulsion (Supporting Information) at 353 K indicate the presence of a small object approximately 5 nm in diameter. One possibility is that these are water droplets; however, modeling these data quantitatively requires calculating the radial electron density distribution $\rho(r)$ of the object. SAXS data of the synthesis mixtures during the first 24 h of synthesis appear essentially identical to the bare microemulsion (Supporting Information). This indicates that over the time frame studied (first 24 h of synthesis) that the silicate species do not appreciably oligomerize to form larger objects. This is consistent with our inability to extract silica particles from these mixtures at synthesis times shorter than 38 h and is also consistent with the idea that the microemsulsion acts to inhibit the growth of silicalite-1 as compared to conventional syntheses.

Effect of Synthesis Temperature. Figure 9 shows how the synthesis temperature impacts the material morphology. Spherical particles are obtained from mixtures of composition 0.2:0.6:0.2 H−S−M (Igepal CO-720) at 353 K. However, above 368 K, the materials possess a more poorly defined morphology at this composition. To obtain spherical particles at higher temperatures, it is necessary to decrease the oil and surfactant content and increase the silicate-1 content to 0.15:0.56:0.29 H−S−M (Igepal CO-720), which produces spheres at both 353 and 368 K (Figure 10). Nitrogen adsorption of the sample obtained at 368 K shows that it possesses a micropore volume of 0.12 cm^3/g. It is also observed by FE-SEM and TEM that the primary particles that comprise the spheres decrease in size from 200 to ~20 nm as the synthesis temperature is decreased (Figure 10) from 368 to 353 K. This is consistent with the PXRD results. So while the size of the spherical particles appears insensitive to the synthesis temperature, the size of the primary particles that comprise them does depend on the synthesis temperature. The heptane/Igepal+butanol/silicalite-1 system yields materi-

(56) Schoeman, B. J. *Stud. Surf. Sci. Catal.* **1997**, *105*, 647−654.

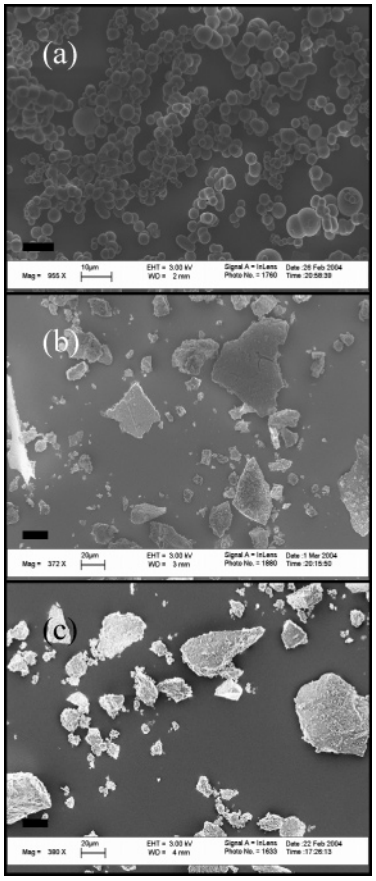

Figure 9. FE-SEM images of silicalite-1 formed at (a) 353 K, (b) 368 K, and (c) 398 K from mixtures of composition 0.2:0.6:0.2 H−S−M, Igepal CO720. Scale bars are (a) 10 μm and (b and c) 20 μm.

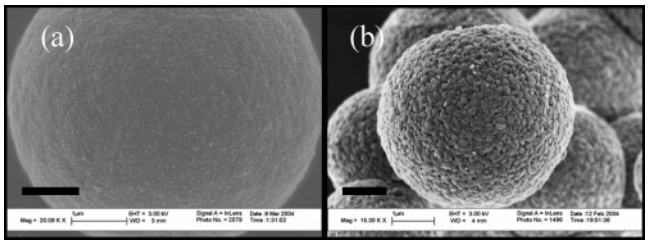

Figure 10. FE-SEM images of silicalite-1 spheres grown at (a) 353 K and (b) 368 K from a mixture of composition 0.15:0.56:0.29 H−S−M, Igepal CO720. Scale bar is 1 μm in both images.

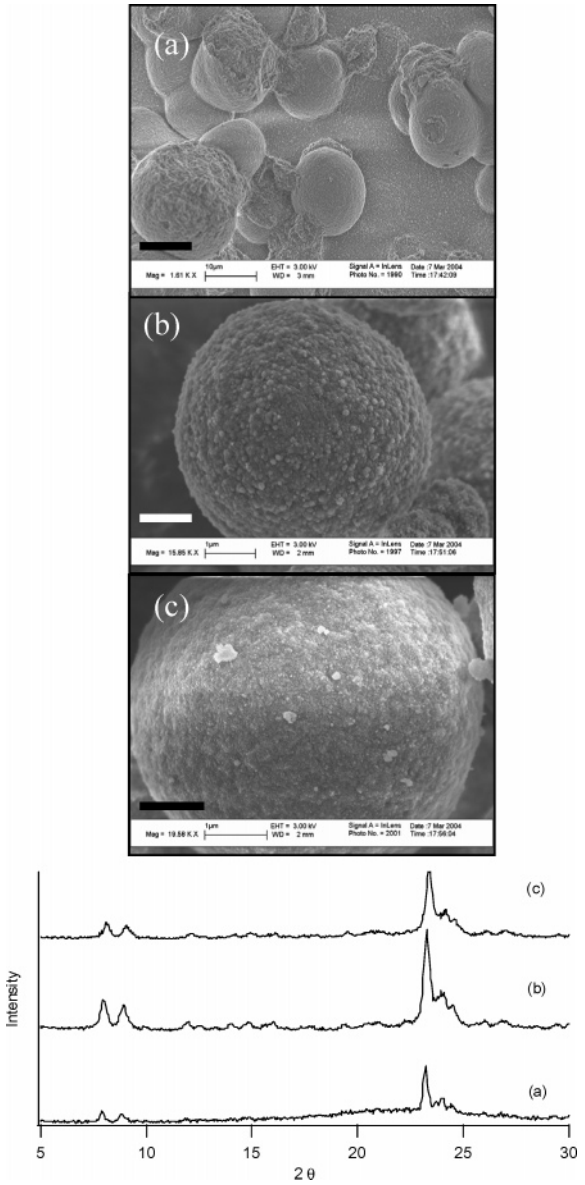

Figure 11. FE-SEM images and XRD data of siliaclite-1 formed in mixtures of composition 0.15:0.425:0.425 H−S−M, surfactant/butanol 2:1 using (a) Igepal- CO520, (b) Igepal-CO720, and (c) Igepal-CO890 at 353 K. Scale bars are (a) 10 μm and (b and c) 1 μm.

als above 373 K that appear essentially identical to those made without the microemulsion, indicating that above 368 K this approach is no longer effective for these mixtures. This result indicates that the surfactant silicate interactions are important in the coalescence process. From correlations between the HLB number and the phase inversion temperature (PIT) of normal heptane/water emulsions with various surfactants, the PIT of Igepal CO-720 (HLB number 14) is approximately 380 K.[48]

Surfactant Identity. The morphology and crystallinity of the silicalite-1 particles is strongly dependent on the structure of the surfactant (Figure 11). The particles synthesized in CO-520 mixtures (0.15:0.425:0.425 H−S−M, surfactant/butanol 2:1) are poorly spherical by FE-SEM and poorly crystalline by PXRD, whereas CO-720 shows highly spherical particles with better crystallinity at the same composition. CO-890 also provides silicalite-1 particles that are spherical. The micropore volumes of these samples are 0.07 cm^3/g (CO-520), 0.10 cm^3/g (CO-720), and 0.11 cm^3/g (CO-890), respectively. The lower micropore volume of the sample made in the presence of the CO-520 is consistent with its poor crystallinity as determined by PXRD. The CO-720 and CO-890 mixtures are two-phase mixtures under these conditions whereas the CO-520 mixture is a one-phase mixture. On the basis of these results, the morphology of the particles is dependent on the number of EO groups in the headgroup, or surfactant identity, suggesting that the surfactant−silicate interactions are responsible for the coalescence of the small particles into large spheres. Another way to understand the results is that surfactants with higher HLB values, and subsequently higher PITs, more readily drive the aggregates to a spherical shape. It was not possible to make platelets with either the CO-720 or CO-890 under any set of conditions, and these surfactants have much higher PITs than the CO-520. As such, it appears that plates can only be

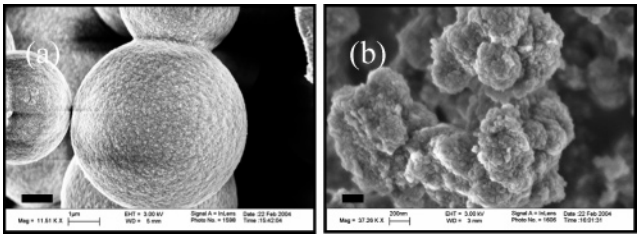

Figure 12. FE-SEM images of silicalite-1 made from mixtures of composition 0.2/0.6/0.2 H−S−M, Igepal CO-720 with a surfactant/butanol ratio of (a) 2:1 and (b) 1:1 at 353 K. Scale bars are (a) 1 μm and (b) 200 nm.

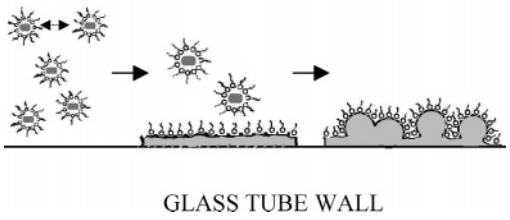

Figure 13. Proposed mechanism for spherical particle formation and growth.

formed above the PIT, whereas spheres are formed below the PIT. It would seem likely that the spherical shape is a consequence of increased surfactant−silicate interactions as the size of the EO headgroup increases.

Surfactant/Cosurfactant Ratio. The morphology of the materials obtained also depends on the ratio of surfactant and butanol. Alcohols are often employed in microemulsions stabilized with nonionic surfactants because they screen the steric repulsions of the hydrophilic headgroups at the interface and result in larger curvatures and higher water solubilization.[57] Figure 12 shows the effect of varying the surfactant/butanol ratio from 1:1 to 2:1 for the Igepal CO-720 system at 353 K (0.2:0.6:0.2 H−S−M). The particles made with a higher ratio are more spherical. So while the butanol may lower the interfacial tension, the morphology is clearly sensitive to the surfactant content. This is again consistent with a surface-mediated process for forming the large zeolite particles. When no butanol is used in this mixture, silicalite-1 materials cannot be recovered.

Proposed Mechanism. Despite the complexity inherent in this system, based on the previous observations we propose the following mechanism for material formation (Figure 13). Initially, the microemulsion acts as a confined space, effectively inhibiting zeolite growth in the early stages of synthesis as compared to bulk syntheses. This is consistent with our inability to extract particles at short synthesis times, as well as our SAXS results. Once the particles reach a critical size, approximately 100 nm based on the results of the sample extracted after a synthesis period of 38 h, it appears that the other aspect of the microemulsion, namely, surfactant adsorption at the silicate surface, becomes important at which stage the small particles formed in the microemulsions aggregate to form large particles. The experiments showing how morphology is influenced by the surfactant content, surfactant identity, and surfactant/butanol ratio all support the hypothesis that it is the surfactants that cause the small particles to aggregate and coalesce. Also, the results indicate that the nature of the surface of the synthesis vessel also strongly influences the shape of the large aggregates obtained.

The materials presented here also differ substantially from the one previous work on silicate-1 growth in microemulsions[33] as well as the other works described in the Introduction. One likely reason for this is that here we employ nonionic surfactants as compared to all the other works in the literature where ionic surfactants are used. The forces between nonionic surfactant and silicate species such as hydrogen bonding are much weaker than electrostatic forces, which will likely dominate in the case of cationic or anionic microemulsions. That we form aggregates of well-defined shapes versus small, dispersed zeolite nanoparticles in the presence of the nonionic microemulsions is consistent with that observation. By contrast, we have performed work using the same zeolite synthesis procedure in cationic microemulsions,[58] and we make materials very different from those reported here.

Conclusions

The synthesis of silicalite-1 in nonionic microemulsions is explored. The results presented demonstrate the ability to manipulate the shape and size of silicalite-1 materials, growing both spheres and high-aspect ratio platelets. In both cases, these large particles are robust aggregates of small submicron particles that are stable to calcination. The size of the primary particles is adjustable based on the synthesis temperature, whereas the size of the large aggregates is adjustable based on the silicalite-1 content of the mixture. On the basis of the results presented, a mechanism is proposed illustrating the role of both the confined space presented by the microemulsion as well as the importance of the surfactant−silicate interactions leading to the formation of the large aggregates. This work suggests this to be a versatile and useful approach for fabricating complex zeolitic materials that possess unique morphological properties and hierarchical structure. Current work is determining whether materials containing heteroatoms such as Al and Ti will possess unusual catalytic properties as a result of their hierarchical structure.

Acknowledgment. The Texas Advanced Research Program and Texas A&M University supported this work. The authors acknowledge the Microscopy and Imaging Center (MIC) at Texas A&M for access to the FE-SEM, SEM, and TEM instrumentation; C. S. Carr for collecting the TEM images; C.-H. Cheng for help with the SAXS measurements; and the X-ray diffraction lab in (TAMU, Chemistry) for access to the PXRD instruments. The FE-SEM instrument was supported by the National Science Foundation under Grant DBI-0116835, and the SAXS instruments were supported by the National Science Foundation under Grant CTS-0215838.

(57) Kahlweit, M.; Strey, R.; Busse, G. *J. Phys. Chem.* **1991**, *95*, 5344−5352.

(58) Axnanda, S.; Shantz, D. F. *Microporous Mesoporous Mater.* **2004**, submitted.

Supporting Information Available: FE-SEM and PXRD of samples made with low heptane contents and low silcalite-1 mixture contents and PXRD patterns of samples shown in Figures 6, 9, 10, and 12; PXRD and FE-SEM of spheres made at 343 K; FE-SEM and PXRD of syntheses performed in Teflon containers with and without a glass slide in the synthesis vessel; and SAXS data for the bare microemulsion and in situ SAXS data on a zeolite synthesis (0.2 H: 0.6 S: 0.2 M, 353 K) (pdf). This information is available free of charge via the Internet at http://pubs.acs.org.

CM0486114